A NEW DIRECT TORQUE CONTROL FOR MINIMIZING THE TORQUE RIPPLE OF INDUCTION MOTOR

Lotfi El M'barki , Moez Ayadi & Rafik Neji

Laboratory of Electronic and Information Technology (LETI) Sfax,
Electric Vehicle and Power Electronics Group (VEEP)
Department of Electrical Engineering, University of Sfax, Tunisia
Email: indtechtunisie@yahoo.fr

ABSTRACT

This paper deals with an improvement based direct torque control (DTC) of an induction motor (IM) and at the same time with on flux and torque of ripples optimizations via each cycle period. The improvement method DTC (IMDTC) is employed on technique switching table, variation of the reference torque error and the judiciously selected of flux error. However of the IMDTC; has large number of selectable voltage vectors in benefit torque ripple reduction, improved quality of IM consumption and it improves the thermal model of the inverter.The proposed method of IMDTC realized by computer simulations.

Keywords: *Minimum torque ripple, IMDTC, RMS, THD, Junction temperature*

1. INTRODUCTION

In the direct torque control of induction motor, the electromagnetic torque and stator flux are used by the selection of a switching vector from table. The minimization of torque ripple and current in IMDTC approach (a, b and c); are used on technique switching vector from table, variation of the torque error and the judiciously selected a fix of flux error [1-8],[11-14],[18-21].

The work application of different approach IMDTC of asynchronous motor, allows by the output of tow hysteresis controllers (torque and flux), with the information of the angular flux location are used to address the switching table. The inverter guards the same state pending the output voltage of the tow hysteresis controllers. For the reason of IMDTC; the voltage switching by minimizing the root-mean-square (RMS) for reducing torque undulation, improve quality of consumption IM [17] while maintaining a constant switching time and improve junction temperature of IGBT. The voltages of the inverter are controlled by the comparisons between the estimated flux and the reference flux it can also be controlled by the comparison of the estimated torque and the reference torque.

The remainder of this paper is organized as follows; model IMDTC of IM is presented in section 2, principle IMDTC is discussed in section3, electrical model of IGBT is presented in section 4, the simulations results and discussions are dealt with in section 5 and the conclusion is presented in section 6.

2. MODEL IMDTC OF IM

The mathematical equations for voltages and fluxes of IM are converted the equations of the three phases IM on the equivalent two-phase components. The equations of IM are given as follows [5].

$$V_{ds} = Rs.I_{ds} + \frac{d\phi_{ds}}{dt} \quad (1)$$

$$V_{qs} = Rs.I_{qs} + \frac{d\phi_{qs}}{dt} \quad (2)$$

$$V_{dr} = Rr.I_{dr} + \frac{d\phi_{dr}}{dt} + W_r\phi_{qr} \quad (3)$$

$$V_{qr} = Rr.I_{qr} + \frac{d\phi_{qr}}{dt} - W_r\phi_{dr} \quad (4)$$

With Vdr = Vqr = 0

$$\phi_{ds} = \int \left(V_{ds} - Rs.I_{ds}\right)dt \quad (5)$$

$$\phi_{qs} = \int \left(V_{qs} - Rs \cdot I_{qs} \right) dt \quad (6)$$

$$\phi_{dr} = \int \left(V_{dr} - Rr \cdot I_{dr} - W_r \phi_{qr} \right) dt \quad (7)$$

$$\phi_{qr} = \int \left(V_{qr} - Rr \cdot I_{qr} + W_r \phi_{dr} \right) dt \quad (8)$$

The absolute value and phase angle of stator flux [18] are given by.

$$\phi_s = \sqrt{\phi^2_{ds} + \phi^2_{qs}} \text{ and } \theta_s = \arctg\left(\frac{\phi_{qs}}{\phi_{ds}} \right) \quad (9)$$

The fluxes and torque can be expressed as.

$$\phi_s = L_s I_s + M I_r \quad (10)$$

$$\phi_r = L_r I_r + M I_s \quad (11)$$

$$T_e = \frac{3}{2} P \phi_s I_s \sin\theta \quad (12)$$

For P = 2 is the number of pole-pairs, Θ is the angle between the stator flux and stator current.

$$T_e = 3 \phi_s I_s \sin\theta \quad (13)$$

The figure 1, the voltage V_{dc} is the DC bus voltage, the commands (S_1, S_2 ,…, S_6) are the inputs signals of model switching table and they are relevant to the IMDTC strategy.

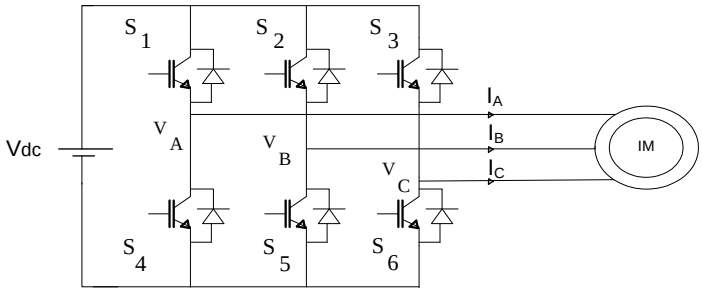

Figure 1. Three- phase voltage inverter.

The voltages (V_A,V_B and V_C) are given by the following matrix.

$$\begin{bmatrix} V_A \\ V_B \\ V_C \end{bmatrix} = \frac{V_{dc}}{3} \begin{bmatrix} 2 & -1 & -1 \\ -1 & 2 & -1 \\ -1 & -1 & 2 \end{bmatrix} \begin{bmatrix} S_1 \\ S_2 \\ S_3 \end{bmatrix} \quad (14)$$

The commands of IGBT (S_1, S_2, or S_3) can be either 1 or 0, the voltage vectors d-q-0 axes are given by the following equations .

$$V_{ds} = \frac{2}{3} V_{dc} \left(S_1 - \frac{1}{2} S_2 - \frac{1}{2} S_3 \right) \quad (15)$$

$$V_{qs} = \frac{2}{\sqrt{3}} V_{dc} \left(\frac{1}{2} S_2 - \frac{1}{2} S_3 \right) \quad (16)$$

The three-phase inverter of eight output states is given by the following equations.

$$V_{di} = V\cos(\frac{\pi}{3}i - \frac{\pi}{3}) \quad , \quad V_{qi} = V\sin(\frac{\pi}{3}i - \frac{\pi}{3}) \tag{17}$$

$$V_i = V_{di} + jV_{qi} \quad , \quad V = \sqrt{\frac{2}{3}}\,V_{dc} \tag{18}$$

with $i = 1,2,...6$; are six non-zero active voltage space vectors.

and $V_0 = V_7 = 0$; are tow zero voltage space vectors.

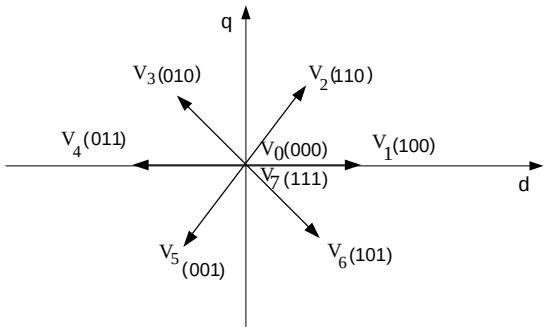

Figure 2. The effect of voltage vectors.

The electromagnetic torque can be rewritten in d-q coordinates as [9],[18].

$$T = \frac{3.P}{2}\left(\phi_{ds}\, I_{qs} - \phi_{qs}\, I_{ds}\right) \tag{19}$$

3. PRINCIPLE IMDTC

The figure 3, the voltages of inverter for tow comparators stator flux and torque are carried out below an approach IMDTC with the optimal switching logic [1-8],[10-12],[14-16],[19]. This method uses a new approach control of torque and flux to minimize the flux and torque ripple. One can indicate that the stator-voltage space vector (Vs) can be used via Vdc and by the switches S_1, S_2 and S_3 as follows.

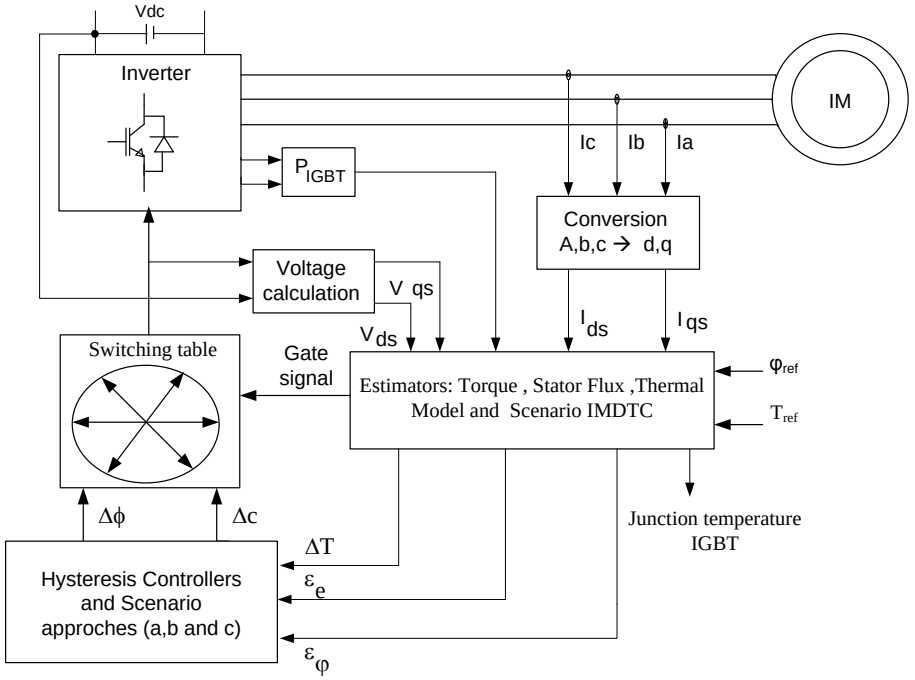

Figure 3. IMDTC principle.

The flux control (ε_φ) is placed in one of the four regions fixed by the following constraints.

$$\phi_{s\max} - \phi_{ref} = \varepsilon_{\varphi_{\max}} \quad , \quad \varepsilon_\varphi \le \varepsilon_{\varphi_{\max}} \tag{20}$$

$$\phi_{s\min} - \phi_{ref} = \varepsilon_{\varphi_{\min}} \quad , \quad \varepsilon_\varphi \ge \varepsilon_{\varphi_{\min}} \tag{21}$$

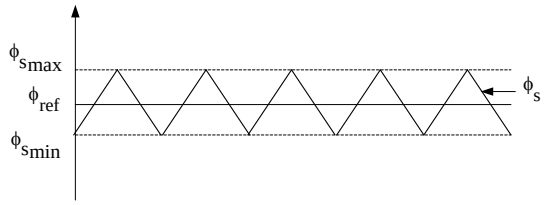

Figure 4. Hysteresis control of flux.

The stator values (flux and current) and rotor flux of the induction motor are determined by the following equations.

$$\begin{bmatrix} \frac{d\phi_S}{dt} \\ \frac{d\phi_r}{dt} \end{bmatrix} = \begin{bmatrix} -\frac{R_S}{H_S} & \frac{mr.R_S}{H_S} \\ \frac{mr.R_r}{H_S} & jWr - \frac{R_r}{\sigma L_r} \end{bmatrix} \begin{bmatrix} \phi_s \\ \phi_r \end{bmatrix} + \begin{bmatrix} 1 \\ 0 \end{bmatrix} V_s \tag{22}$$

$$I_s = \frac{\phi_s - m_r \phi_r}{H_s} \tag{23}$$

For $H_s = L_s.\sigma$ and $m_r = \frac{M}{L_r}$

The torque is given by the following equation [15],[19],[21].

$$T_e = \frac{3}{2}\frac{p.m_r}{H_s}\phi_s \phi_r \sin(\theta_s - \theta_r) \tag{24}$$

The angle between the stator flux and rotor flux; is critical role in scheming output torque.

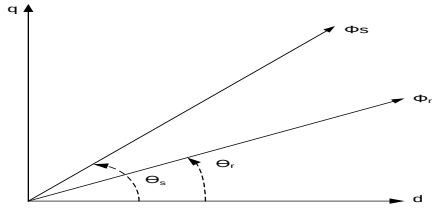

Figure 5. The principle of stator flux and rotor flux.

The rotor and stator fluxes of equation (22) are expressed in the discrete form as [3].

$$\phi_{s(k+1)} = \phi_{sk} + \left(-\frac{R_S}{H_S}\phi_{sk} + \frac{mr.R_S}{H_S}\phi_{rk} + V_{sk} \right).t_{cp} \tag{25}$$

$$\phi_{r(k+1)} = \phi_{rk} + \left(\frac{mr.R_r}{H_S}\phi_{sk} + \left(jWr - \frac{R_r}{\sigma.L_r} \right)\phi_{rk} \right).t_{cp} \qquad (26)$$

With k+1 is sampled instant and t_{cp} controlling period of a small value. The work application of proposed technique, provoke the improvement RMS torque ripple for trimming of torque ripple. The torque and flux errors ($\varepsilon_{e,}$ ε_{φ}) are realized by tow hysteresis controllers and alters their outputs at the cycling period. For the reason of IMDTC; the voltage switching by reducing the RMS for minimizing torque undulation while maintaining a constant switching frequency. The torque control (ε_e) is placed in one of the four regions fixed by the following constraints [3].

$$T_{e.max} - T_{ref} = \varepsilon_{e_{max}} \quad , \quad \varepsilon_e \le \varepsilon_{e_{max}} \qquad (27)$$

$$T_{e.min} - T_{ref} = \varepsilon_{e_{min}} \quad , \quad \varepsilon_e \ge \varepsilon_{e_{min}} \qquad (28)$$

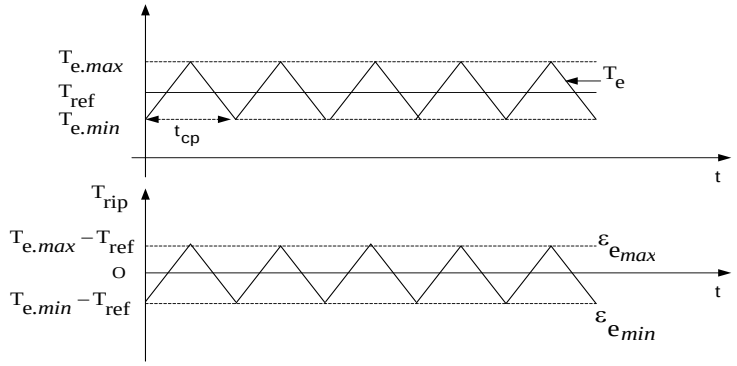

Figure 6. Hysteresis control of torque and torque ripple (T_{rip}).

For t_{cp} is the controlled period of a small value. The minimization of torque ripple in IMDTC is used on technique switching vector from table1 and the output signal gate of the voltage switches of the inverter.

.

sector		1	2	3	4	5	6
Flux	Torque						
$\Delta\phi = 1$	$\Delta c = 1$	V_2	V_3	V_4	V_5	V_6	V_1
	$\Delta c = 0$	V_0	V_7	V_0	V_7	V_0	V_7
	$\Delta c = -1$	V_6	V_1	V_2	V_3	V_4	V_5
$\Delta\phi = 0$	$\Delta c = 1$	V_3	V_4	V_5	V_6	V_1	V_2
	$\Delta c = 0$	V_7	V_0	V_7	V_0	V_7	V_0
	$\Delta c = -1$	V_5	V_6	V_1	V_2	V_3	V_4

Table 1. Switching table for conventional DTC

The root-mean-square (RMS) torque ripple is a one by sampling number (n) of the RMS value with Te ripple between $T_{e.max}$ and $T_{e.min}$. The RMS value channel provoking in a sampling number via inputs of torque ripple. In other, the RMS value of the torque ripple (T_{rip}) can be expressed as follows.

$$RMS\left(T_{rip} \right) = T_{ripr} = \sqrt{\frac{1}{n}\sum_{i=1}^{n}\left(\varepsilon_{ei}\right)^2} \qquad (29)$$

RMS (T_{rip}) is calculated the RMS value of each column in the torque ripple, or detects the RMS value of an order of inputs over a period.

$$T_{ripr} = \sqrt{\frac{1}{n} \sum_{i=1}^{n} \left(T_{ei} - T_{ref} \right)^2} \quad (30)$$

The RMS in term of flux ripple is given by the following equation.

$$\varepsilon_{\varphi ripr} = \sqrt{\frac{1}{n} \sum_{i=1}^{n} \left(\varepsilon_{\varphi i} \right)^2} \quad (31)$$

The total harmonic distortion (THD) is defined as the RMS value of the fundamental current (I_f) and RMS value of the harmonic (I_K). The quality IMDTC of IM is measured with the total harmonic distortion (THD_I) for the phase current.

$$THD_I = \frac{I_K}{I_f} \quad \text{with} \quad I_K = \sqrt{I_2^2 + I_3^2 + ...+ I_K^2} \quad (32)$$

The histeresis controller for uncertainty torque (ΔT) is ordered by reference torque (T_{ref}).

.

$$\Delta T = \frac{X.T_{ref}}{100} \ , \ \text{with} \ \ \Delta T \in \left[\varepsilon_{e\min} , \varepsilon_{e\max} \right] \quad (33)$$

The IMDTC realizes to make the instantaneous torque equal with the reference torque at the end of the cycle and these principles are given by the following equations.

$$Te(k+1) \cong T_{ref} \quad (34)$$

$$\text{Case (a);} \ \lim \Delta T_{X \to 20} = 8 \, \text{N.m} \quad (35)$$

$$\text{Case (b);} \ \lim \Delta T_{X \to 10} = 4 \, \text{N.m} \quad (36)$$

$$\text{Case (c);} \ \lim \Delta T_{X \to 0.1} = 0.04 \, \text{N.m} \quad (37)$$

The torque estimation (Te) and electromagnetic torque (T) of IM are given by the following equation.

$$\frac{Te}{T} = 1 \quad (38)$$

4. ELECTRICAL MODEL OF IGBT

Thermal model of IGBT is employed to estimate the maximum junction temperature of the module. A system of cooling is not employed for IGBTs. The electric model used for the Semikron module SKM 75GB 123D of IGBT at various temperatures; the voltage drop at the boundaries ($V_{CEsat(t)}$), with power dissipated (P_{dis}) and internal resistance ($R_{CE(Tj)}$) can be expressed by the following equations [22],[23].

$$P_{dis\,(t)} = V_{CE(Tj)} \cdot I_{c\,(t)} + R_{CE(Tj)} \cdot I^2_{C\,(t)} \quad (39)$$

$$V_{CE(Tj)} \leq 1{,}5 + 0{,}002.(T_j - 25) \quad (40)$$

$$0{,}00008.(T_j - 25) + 0{,}020 \leq R_{CE\,(Tj)} \leq 0{,}030 + 0{,}00010.(T_j - 25) \quad (41)$$

5. SIMULATIONS RESULTS AND DISCUSSIONS

The control system of an IMDTC induction motor utilizes a two-level controller, for histeresis flux and histeresis torque.These controls torque and stator flux, are used by the selection of a switching vector via table 1 and table 2 for improving the torque ripple by approaches method DTC. With IMDTC is determined enters the two basic variables Δc and $\Delta\phi$ for table 3 and table 2 represents the results of three approaches IM.

.

Cases	a	b	c
X	20	10	0.1
ΔT (N.m)	8	4	0.04

Table2. Improving the torque ripple by approaches

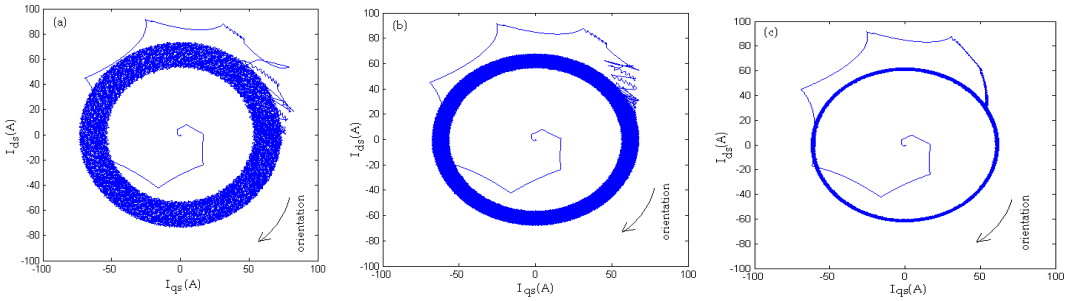

Figure 7. Improvement state response of currents (I_{ds} and I_{qs}).

The figure 7, illustrate amelioration the minimum current ripple of IMDTC. The response current form in interior and out the circle is presented the current during startup of the motor. The response currents (I_{ds} and I_{qs}) out of the circle: in the approach (a) at $t(s) =]0.002, 0.008[$; the current during startup of the motor equal 95.5A, with the approach (b) at $t(s) =]0.002, 0.008[$; the current during startup of the motor equal 95A and in the approach (c) at $t(s) =]0.002, 0.008[$; the current during startup of the motor equal 92A. Therefore, in the figure 7 of approaches (a, b and c) for the response current form in interior of the circle at $t(s) = [0.000, 0.002]$; the current during startup is lower current after startup of the motor. They also show that the current-error lies below and above the circle with maintain the steady-state operation and orientation of currents (I_{ds} and I_{qs}). The approach (c) of figure 7 compared with the figure 7.a or figure 7.b; achieve a faster torque response and the currents (I_{ds} and I_{qs}) ripples are much reduced.

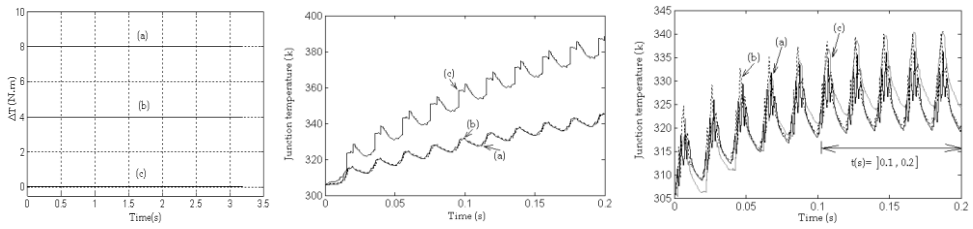

(a1) (a2) (a3)

Figure 8. Approaches results; (a1). Improvement torques control by approaches, (a2). Evolution of the junction temperature (in the IGBT1) and (a3) . Evolution after cooling of the junction temperature (in the IGBT1).

The figure 8.a1, via ΔT, provoke the large number of selectable voltage vectors, it benefit reduce torque and current ripples of IM. Because of the IMDTC, is determined with the offset torque (ΔT); case (a), equal 8 N.m with case (b), equal 4 N.m and case (c), equal 0.04 N.m. The figure 8 (a2 and a3), Thermal Semikron module SKM 75GB 123D of IGBT is employed to estimate the maximum junction temperature of the module. The cases IMDTC were followed in a precise method of figure 3. The estimated torque, the same as the electromagnetic torque IM and the reference torque (40 Nm) are used in application of scenario IMDTC. For figure 8, the maximum junction temperature at 0.1s via approaches DTC; case (a), equal 331.636 K with case (b), equal 332.051 K and case (c), equal 362.089 K. Consider the result; it is necessary to employ a system of cooling for IGBTs. For equations (39-41) determining after

cooling of the new junction temperature (T_{jN}). The actual junction temperature; T_{j1} of cases (a and b) and T_{j2} of case (c), with the temperature of cooling (T_{jc}) are given by the following equations.

$$\text{Cases (a and b); } T_{jN} = T_{j1} - T_{jc} \quad (42)$$

According to figure 8.a3, the junction temperature after cooling of approach (c) equal to the junction temperatures of the approaches (a and b), it is necessary to make.

$$\text{Case (c); } T_{jN} = T_{j2} - 2T_{jc} \quad (43)$$

For equations (42) and (43), with t(s) = $]0.1,0.2\ ]$; the average junction temperature after cooling (T_{jN}) of the cases (a,b and c) is almost at 330K.

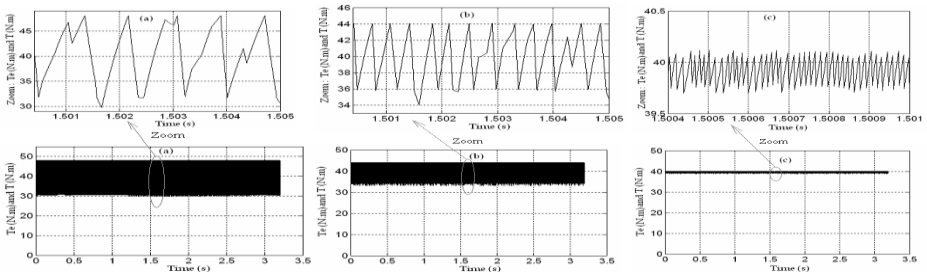

Figure 9. Improvement of the torque undulation .

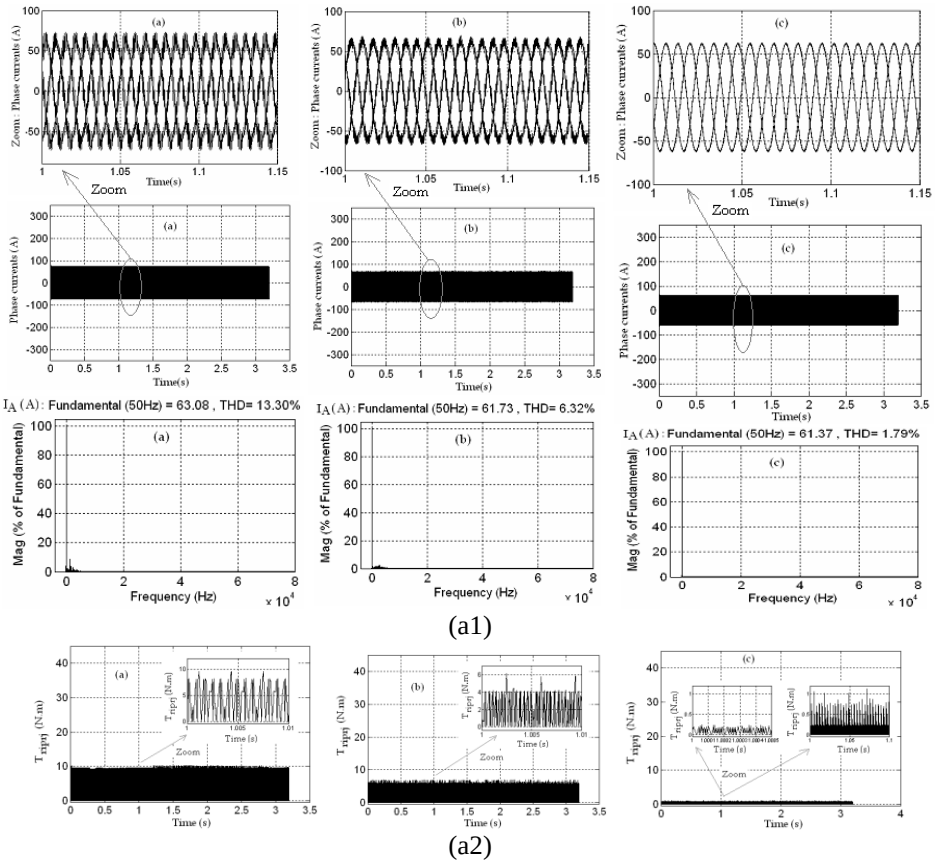

(a1)

(a2)

Figure 10. IMDTC of approaches results for a load of 40 Nm; (a1) Improvement of the currents and (a2) Improvement of the RMS torque ripple.

The figure 9 and figure 10, represents ameliorations respectively the minimum ripple DTC, the total harmonic distortion, RMS torque ripple, and currents of three approaches (a, b and c). The idea is improved the DTC by the histeresis controllers (torque and flux) and modification voltage space vector.

Figure.10.a1, in case (a) shows the input current of IM and harmonic spectrum of inverter with the THD of current is 13.30 % by 63.08 A.The THD current is 1.79 % with 61.37 A, as illustrated in figure.10.a1 of case (c), this shows

excellent performance in the low harmonic spectrum. The phase current with of approach (c) allows minimizations in output current total harmonic distortion and the torque ripple. The technique IMDTC of induction motor in figure 3, is realized with different cases (a, b and c) of table 3 and the figure 10 of approaches results; recapitulate advantages of the IMDTC for the induction motor. We have according to the figure 10.a2 of case c an approximately 97% reduction in RMS torque ripple in IMDTC.

Results IMDTC	a	b	C
ΔT (N.m)	8	4	0.04
Reduction (%) , RMS$\left(T_{rip} \right)$ (N.m)	Nothing	60	97
THD (%)	13.30	6.32	1.79
I_A (A)	63.08	61.73	61.37
Junction temperature (K) in the IGBT1 at 0.2s	345,325	345,561	390,520
Average junction temperature after cooling (K) in the IGBT1 at t(s) = $]0.1,0.2]$	330	330	330

Table 3. The results IMDTC of the induction motor for a load of 40 Nm.

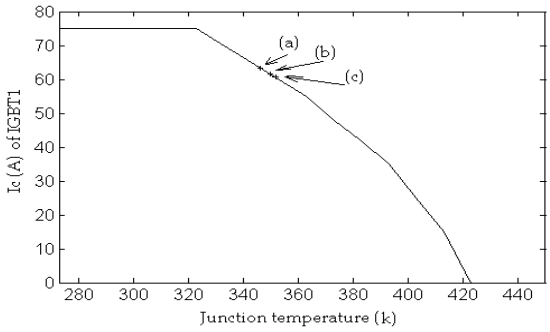

Figure 11. Rated current Ic to junction temperature of module SKM 75GB 123D.

According to the passage current Ic of thermal Semikron module SKM 75GB 123D (IGBT1) via function to the junction temperature, one can place currents IA of the approaches (a,b and c); provoke the maximum junction temperature which can support IGBT are given by the following table 4.

.

module SKM 75GB 123D	a	b	C
I_C (A) equal I_A (A) in our case	63.08	61.73	61.37
The maximum junction temperature of IGBT1 (K)	346.84	349.53	350.26

Table 4. The results of module SKM 75GB 123D

With the figure 11 and table 4, the effectiveness of our system of temperature cooling is revealed because the junction temperature of IGBT is 330 k in the different cases (a, b and c), which can carried the current 71.5 A of figure 11. According to the figure 10.a1, our currents are lower than 71.5 A, implies that module SKM 75GB 123D (IGBT1) function in good condition of consummation currants. For better results, one can reduce the junction temperature of IGBT

R_s: Stator resistance (1.4534 Ω), R_r: Rotor resistance (1.4160 Ω), L_r: Rotor inductance (0.0143H), L_s: Stator inductance (0.0144H), M: Mutual inductance (0.0132H), V_{ds}, V_{qs}: d-axis and q-axis stator voltages, I_{ds}, I_{qs} : d-axis and q-axis stator currents, $\sigma = 1 - \frac{M^2}{Lr.Ls}$: Blondel coefficien t, Φ_r: Rotor Flux, Φ_s : Stator flux,	T_r: Load of torque (40 N.m), T: Electromagnetic torque, Te: Torque estimator, T_{ref} : Reference torque, F: Friction coefficient (0.015 kg.m² /S), J: Moment of inertia (0.312 kg.m²), p : Number of pole pairs in the motor (2), f : Fundamental frequency (50 Hz), V_{dc}: Continuous tension (460V), tsp: Small control period, ωr : Rotor pulsation, (k +1) : Sample instant.

Table 5. List of Symbols.

6. OVERALL CONCLUSIONS

The paper presents comparison approaches via advantages of table 2 and table 3 applied to the IMDTC of asynchronous machine with development of temperature switching IGBT. The technique of IMDTC induction motor in figures (7-11) has been realized with different cases (a, b and c). The application IMDTC of induction motor, allows by using hysteresis controllers to regulate torque and flux with the information of the angular location, is used to address the switching table. The IMDTC allows minimizations in output current total harmonic distortion and the torque ripple. The advantage table 3 realizes the input current, shows the lowest harmonic and minimizes the torque ripple. For the case c, it can be seen that the overall performance of technique method of the IMDTC system is much improved, compared with the approaches (a and b). According to the results from the junction temperature of table 3, one can minimize the temperature of cooling to reduce the junction temperature of IGBT.

7. ACKNOWLEDGEMENTS

The authors would thank ENIS-Tunisia, FSG-Tunisia, and ESSTT-Tunisia for the helpful support in the work.

8. REFERENCES

[1]. M. Depenbrock, "Direct self-control (DSC) of inverter-fed induction machine" ,IEEE Trans. Power Electron., vol.3, pp. 420-429, Oct.1988.

[2]. Salih Baris Ozturk, and Hamid A. Toliyat,," Direct Torque and Indirect Flux Control of Brushless DC Motor", IEEE/Asme Transactions on Mechatronics,2010, This article has been accepted for inclusion in a future issue of this journal. Content is final as presented, with the exception of pagination, p10.

[3]. Kuo-Kai Shyu, , Juu-Kuh Lin, Van-Truong Pham, Ming-Ji Yang, and Te-Wei Wang, "Global Minimum Torque Ripple Design for Direct Torque Control of Induction Motor Drives", IEEE Transact. Ind. Elec, VOL. 57, No.9, September 2010,pp 3148-3156.

[4]. Yongchang Zhang, Jianguo Zhu," Direct Torque Control of Permanent Magnet Synchronous Motor with Reduced Torque Ripple and Commutation Frequency", Copyright (c) 2010 IEEE, This article has been accepted for publication in a future issue of this journal, but has not been fully edited. Content may change prior to final publication,pp 1-14.

[5]. Auzani Jidin, Nik Rumzi Nik Idris, Abdul Halim Mohamed Yatim, , Tole Sutikno, Malik E. Elbuluk, "An Optimized Switching Strategy for Quick Dynamic Torque Control in DTC Hysteresis-Based Induction Machines", 2010 IEEE, This article has been accepted for publication in a future issue of this journal, but has not been fully edited. Content may change prior to final publication,p 9.

[6]. Bekheira Tabbache, Abdelaziz Kheloui and Mohamed Benbouzid," An Adaptive Electric Differential for Electric Vehicles Motion Stabilization", This article has been accepted for publication in a future issue of this journal, but has not been fully edited. Content may change prior to final publication,p8.

[7]. I. Takahashi and Y.Ohmori, "High performance Torque Control of year Induction Motor", IEEE Transactions one Industry Applications, vol. 25, pp. 257-264, March/April 1989.

[8]. Gabriel Cimuca, Stefan Breban, Mircea M. Radulescu,Christophe Saudemont, and Benoit Robyns," Design and Control Strategies of an Induction-Machine-Based Flywheel Energy Storage System Associated to a Variable-Speed Wind Generator", IEEE Trans.on Ener.Conv.,Vol .25,No.2,June2010,pp 526-534.

[9]. Zhifeng Zhang, Renyuan Tang, Baodong Bai, and Dexin Xie," Novel Direct Torque Control Based on Space Vector Modulation With Adaptive Stator Flux Observer for Induction Motors", IEEE Transactions one Magnetics, Vol. 46, No. 8, August 2010,pp 3133- 3136.

[10]. Kyo-Beum Lee, Sung-Hoe Huh, Ji-Yoon Yoo, and Frede Blaabjerg, ," Performance Improvement of DTC for Induction Motor-Fed by Three-Level Inverter With an Uncertainty Observer Using RBFN '', IEEE Trans. on Energy Conv, vol.20.no.2,Janury 2005. pp. 276- 283.

[11]. Joon Hyoung Ryu, Kwang Won Lee, and Ja Sung Lee," A Unified Flux and Torque Control Method for DTC-Based Induction-Motor Drives", IEEE Trans. on Power Electron., vol.21.no.1, Janury 2006. pp. 234 - 242.

[12]. Yongchang Zhang, Jianguo Zhu, Wei Xu, and Youguang Guo, "Simple Method to Reduce Torque Ripple in Direct Torque Controlled Permanent Magnet Synchronous Motor by Using Vectors with Variable Amplitude and Angle",IEEE.2010, This article has been accepted for publication in a future issue of this journal, but has not been fully edited. Content may change prior to final publication.,p12.

[13]. Liliang Gao, John E. Fletcher and Libo Zheng," Low Speed Control Improvements for a 2-level 5-phase Inverter-Fed Induction Machine Using Classic Direct Torque Control", IEEE 2010,This article has been accepted for publication in a future issue of this journal, but has not been fully edited. Content may change prior to final publication.p10.

[14]. Farid Khoucha, Mouna Soumia Lagoun, Abdelaziz Kheloui and Mohamed El Hachemi Benbouzid," A Comparison of Symmetrical and Asymmetrical Three-Phase H-Bridge Multilevel Inverter for DTC Induction Motor Drives", IEEE Transact. On Enrg..Conv.,2010, This article has been accepted for inclusion in a future issue of this journal. Content is final as presented, with the exception of pagination.p.9.

[15]. M. Aktas V. Turkmenoglu, ,'' Wavelet-based switching faults detection in direct torque control induction motor drives", IET Sci. Meas. Technol., 2010, Vol. 4, Iss. 6, pp. 303–310.

[16]. Jef Beerten, Jan Verveckken, and Johan Driesen," Predictive Direct Torque Control for Flux and Torque Ripple Reduction", IEEE Transact. On Ind. Elec, Vol.57, No.1 January 2010, pp 975- 985,pp.404- 412.

[17]. Masood Hajian, Jafar Soltani, Gholamreza Arab Markadeh, and Saeed Hosseinnia" Adaptive Nonlinear Direct Torque Control of Sensorless IM Drives With Efficiency Optimization", IEEE Transact. On Ind. Elec, Vol.57, No.3 March 2010, pp 975- 985.

[18]. Giuseppe Buja, and Roberto Menis, " Steady-State Performance Degradation of a DTC IM Drive Under Parameter and Transduction Errors", IEEE Transact. On Ind. Elec, Vol.55, No.4 April 2008 ,pp 1749-1760.

[19]. Yongchang Zhang, Jianguo Zhu, Zhengming Zhao, Wei Xu, David G. Dorrell, "An Improved Direct Torque Control for Three-Level Inverter-Fed Induction Motor Sensorless Drive", This article has been accepted for publication in a future issue of this journal, but has not been fully edited. Content may change prior to final publication,IEEE Trans.Power Electron., vol.21.no.5, November2010.pp1-12.

[20]. Saad Sayeef, Gilbert Foo, and M. F. Rahman, "Rotor Position and Speed Estimation of a Variable Structure Direct-Torque-Controlled IPM Synchronous Motor Drive at Very Low Speeds Including Standstill", ", IEEE Transact.On Ind. Elec, Vol. 57, No.11,November2010 ,pp 3715-3723.

[21]. Farid Khoucha, Soumia Mouna Lagoun, Khoudir Marouani, Abdelaziz Kheloui, and Mohamed El Hachemi Benbouzid, "Hybrid Cascaded H-Bridge Multilevel-Inverter Induction-Motor-Drive Direct Torque Control for Automotive Applications", IEEE Transact.On Ind. Elec, Vol.57, No.3 March 2010 ,pp 892- 899.

[22]. Moez Ayadi, Mohamed Amine Fakhfakh, Moez Ghariani and Rafik Neji, " Electrothermal modeling of hybrid power", Microelectronics International, vol. 27. n. 3, August 2010, pp. 170-177.

[23]. Moez Ayadi, Mohamed Amine Fakhfakh, Moez Ghariani and Rafik Nej, Electro-Thermal Simulation of a Three Phase Inverter with Cooling , Journal of Modelling and Simulation of Systems, vol. 1. n. 3, 2010, June 2010, pp. 163-170.